Q: 2 3 4 5

Hematite reconstruction of Late Triassic hydroclimate over the olorado Plateau

Christopher J. Lepre[a,1] and Paul E. Olsen[b,c]

[a]Department of Earth and Planetary Sciences, Rutgers University, NJ; [b]Lamont-Doherty Earth Observatory, Columbia University, NY; and [c]Department of Earth and Environmental Sciences, Columbia University, NY

Edited by Lisa Tauxe, University of California, San Diego, La Jolla, CA, and approved January 6, 2021 (received for review March 9, 2020)

Hematite is the most abundant surficial iron oxide on Earth resulting from near-surface processes that make it important for addressing numerous geologic problems. While red beds have proved to be excellent paleomagnetic recorders, the early diagenetic origin of hematite in these units is often questioned. Here, we validate pigmentary hematite pigmentite") as a proxy indicator for the Late Triassic environment and its penecontemporaneous origin by analyzing spectrophotometric measurements of a 14.5-My–long red bed sequence in scientific drill core CPCP-PFNP13-1A of the Chinle Formation, Arizona. Pigmentite concentrations in the red beds track the evolving pattern of the Late Triassic monsoon and indicate a long-term rise in aridity beginning at 215 Ma followed by increased oscillatory climate change at 213 Ma. These monsoonal changes are attributed to the northward drift of the Colorado Plateau as part of Laurentia into the arid subtropics during a time of fluctuating CO_2. Our results refine the record of the Late Triassic monsoon and indicate significant changes in rainfall proximal to the Adamanian–Revueltian biotic transition that thus may have contributed to apparent faunal and floral events at 216 to 213 Ma.

hematite monsoon red beds Triassic Pangaea

Q:6 Hematite is usually represented by two phases in rocks, sediments, and soils. One is specularite, with opaque, relatively large, and commonly euhedral crystals. The other is a fine-grained, often poorly crystalline phase that provides most of hematite s characteristic color. Both are capable of carrying a magnetic remanence, yet each has a separate characteristic magnetic coercivity and thermal unblocking spectra 1, 2). Specularite crystals typically yield a red streak on porcelain plates that cause the mechanical breakdown of the sample into small particles: grains with diameters less than 100 nm are generally orange, those of about 500 nm are red, and sizes around 1,500 nm appear dark purple 3). Visible light reflectance increases and wavelengths get shorter as hematite grain size becomes smaller, with changes from yellow-red to blue-red accompanying increasing diameter 4). The magnetic behavior of iron oxides is viscous/unstable with decreasing grain size, and thus, ultrafine 100 nm) hematite is perhaps unreliable for paleomagnetic studies 5, 6).

Understanding the origins of these minerals and their timing of formation within geologic units has been an ongoing pursuit, and the study of North American red beds has been instrumental to such inquiries 7–10). Some research has long suggested that red bed color has had a protracted geologic history and hematite was formed considerably after the deposition of the host rock 11). The usefulness of hematite in red beds as a paleoclimate indicator at the time of deposition, or as a carrier of a penecontemporaneous record of the Earth s magnetic field, is thus impaired if the hematite formed much later in time through diagenetic alteration 12). Similarly, red bed paleomagnetic remanence has been argued to have been acquired through a chemical remanent magnetization that postdates deposition by millions or tens of millions of years 13, 14). However, Triassic–Jurassic hematite-bearing red shales, mudstones, and siltstones as well as magnetite-bearing gray-to-black shales) of the Newark Basin record magnetozones that represent the polarity of the geomagnetic field close to the time of deposition, as shown by internal comparisons of magnetizations and 20-ky–level cyclostratigraphy 15). This study along with others suggests that thermal unblocking patterns of coercivity spectra demonstrate the contribution of detrital specularite to the characteristic remanence, whereas the red pigment phase has been shown to carry a paleomagnetic overprint 1, 2, 7, 9, 16). This has supported the idea that the colorization of the red beds derives from a secondary diagenetic product, formed sometime after the specularite acquired characteristic remanence. Newark Basin–wide lake cycles and polarity magnetozones occur in consistent mutual stratigraphic relationships at different sites separated by 4 to 42 km and crosscut red-gray color boundaries 17) reflecting specular hematite versus magnetite remanence 15). Recent tests of these interpretations using hematite-bearing red beds of the Chinle Formation further support a very early acquisition of the characteristic magnetizations by the specularite 18, 19). However, color changes of the Newark Basin red beds have been correlated with sedimentary and moisture cycles that were caused by orbital climate forcing of the Late Triassic monsoon 8). This insinuates that at least some of the pigmentary hematite is indeed ancient and may provide a record of how hydrated a past soil environment was, relating to rainfall.

Red beds of the Chinle Formation of the Colorado Plateau in Arizona Fig. 1) are one of the most geographically exposed Late Triassic terrestrial sedimentary archives of western Pangaea. These deposits preserve the Adamanian–Revueltian biotic turnover, involving the largest magnitude faunal and floral change on land during all but the final part of the Late Triassic

Significance

Hematite provides much of the color for the classic Triassic–Jurassic red beds" of North America and elsewhere. Measuring the spectrum of visible light reflected and absorbed by the red beds, we demonstrate that the hematite concentrations faithfully track 14.5 million years of Late Triassic monsoonal rainfall over the Colorado Plateau of Arizona and use this information to assess interrelationships between environmental perturbations, climate, and the evolution of terrestrial vertebrates. The research challenges conventional ideas that the hematite has limited use for interpreting the ancient past because it is a product of natural chemical alterations that occurred long after the beds were initially deposited.

Author contributions: C.J.L. designed research, performed research, and collected data; C.J.L. and P.E.O. analyzed and interpreted data and wrote the paper.

The authors declare no competing interest.

This article is a PNAS Direct Submission.

[1]To whom correspondence may be addressed. Email: clepre@eps.rutgers.edu.

This article contains supporting information online at https://www.pnas.org/lookup/suppl/doi:10.1073/pnas.2004343118/-/DCSupplemental.

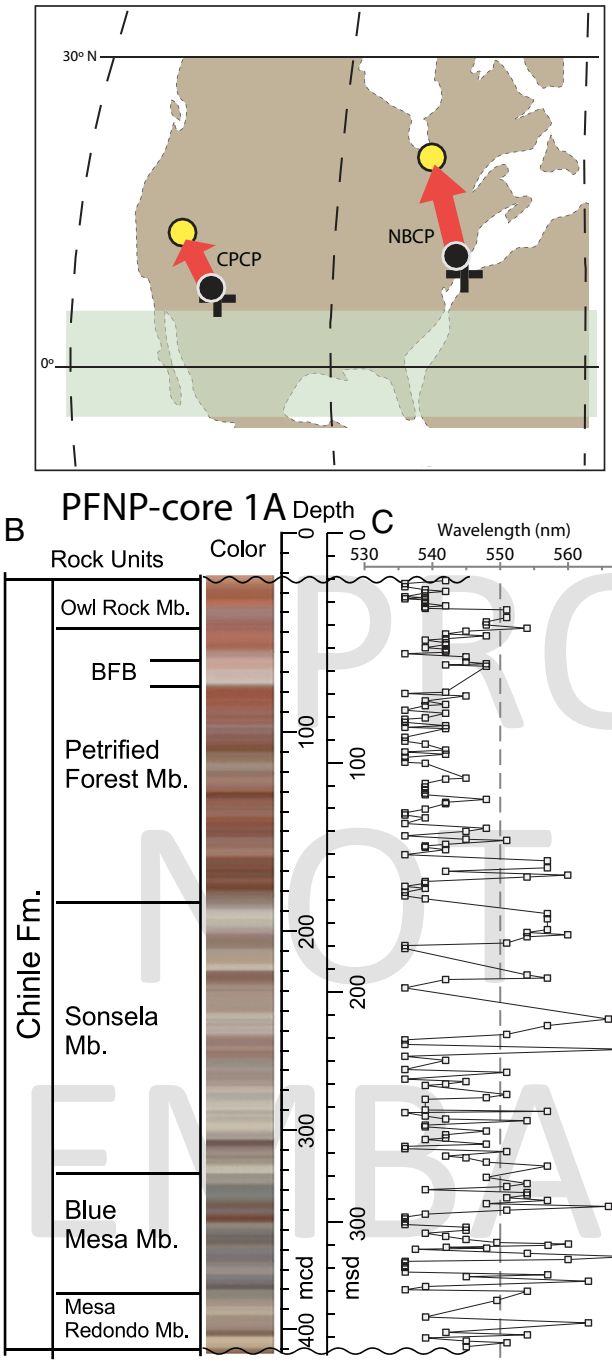

Fig. 1. (*A*) Pangaean geography according to a 220-Ma mean composite paleopole (56) with the Chinle Formation (CPCP, Colorado Plateau Coring Project) and the Newark Basin (NBCP, Newark Basin Coring Project) indicated by filled circles connected by arrows to their relative positions at 200 Ma by open circles (25). (*B*) Lithostratigraphic unit names, predominant colors, and thickness of the Chinle Formation in PFNP-core 1A (18, 19, 25). (*C*) DRS results showing changes of the position of the characteristic absorption band for hematite. Note the very good agreement between the red (purple) colors of the core and wavelengths 550 nm (>550 nm).

20, 21). Although magneto-chronostratigraphic evidence constrains the Adamanian–Revueltian turnover to 216 through 213 Ma 18), its cause and rapidity is still open to debate 22–24).

We studied mudstones of the Chinle Formation in scientific drill CPCP-PFNP13-1A hereafter PFNP-core 1A) Fig. 1*B*) drilled at Chinde Point of the Petrified Forest National Park of Arizona in the United States 25). Chinle mudstones are overprinted with paleosols and thought to have been developed within a fluvial floodplain depositional environment 22, 25, 26). We acquired diffuse reflectance spectroscopy DRS) measurements from these paleosol-bearing mudstones to evaluate the controls on hematite production within the ancient soils. Hematite variations registered to the core chronostratigraphy provide details on the timing of monsoonal rainfall changes that can be compared with other records to reconstruct the environmental history of Late Triassic age strata of the Colorado Plateau Fig. 2).

Materials and Methods

The Late Triassic Chinle Formation is largely a record of fluvial deposits accumulated within a shallow basin originating as a back-bulge of the Cordilleran Arc or postrift passive margin wedge as reviewed in ref. 25. PFNP-core 1A samples a 335-m–thick stratigraphic succession of nearly all of the Chinle preserved in the park, including the lower Owl Rock, Petrified Forest, Sonsela, Blue Mesa, and Mesa Redonda members (Fig. 1*B*). Floodplain paleosols within the core are overprinted on fluvio-lacustrine mudstones that are recognized by the presence of one or more pedogenic features (i.e., carbonate nodules, slickensides, and clayey and calcified root traces) and elimination of primary depositional structures such as bedding and ripples. Levels displaying clear depositional sedimentary structures or well-sorted sands were not sampled for DRS study. Paleosols in the Chinle Formation are largely Inceptisols and Vertisols; however, there is no monotonic change in paleosol-type up-section, yet Vertisols are common to the Blue Mesa Member and Aridsols to the Owl Rock (22, 26, 27). Supporting information for interpreting the hematite content of the paleosols in the core has been collected from published studies of the Chinle outcrops (Fig. 2*C*). Although registry to the cores is not perfect (18, 28), these outcrop studies provide bulk geochemical analyses of paleosol types identified in the Petrified Forest National Park study area. The data represent a chemical index of alternation minus the potassium content (CIA-K) that has been parameterized to serve as a proxy record of mean annual rainfall for the Late Triassic Colorado Plateau (22, 26).

Chronostratigraphy of PFNP-core 1A (Fig. 2*A*) has been established previously by high-precision U-Pb dates on detrital zircons and independently Q:7 by magnetostratigraphic correlations with the time scale of the Newark–Hartford basins of the northeast United States (18, 19) that are consilient. The working half of PFNP-core 1A was studied at the Rutgers University Core Repository, Livingston Campus (Pitscataway, New Jersey). We conducted DRS measurements of hematite concentrations on 197 separate levels, from a stratigraphic depth of 21 to 354 m (*SI Appendix*, Table S2). The sampled levels have a median stratigraphic spacing of 1.3 m, and 90 of the 197 levels were spaced between 0.3 and 3.0 m. DRS measurements were taken on the core face with an integrating sphere, fiber-optically fitted to a Varian-Cary 50 UV-Vis spectrophotometer. Experimental conditions are described in detail in ref. 29. Hematite s double electron excitation of the magnetically spin-coupled Fe ions within the crystal lattice makes its characteristic wavelength band almost unique as compared to other iron oxides (30). This phenomenon is referred to as the electron pair transition at a peak position between 535 and 580 nm (31, 32). The amplitude of the peak in the second derivative curve was used to interpret the hematite concentration of the paleosols (*SI Appendix*, Fig. S1 and Table S1).

Results

Hematite s characteristic absorption band varies at 535 to 570 nm in the lower part of the core but changes to almost exclusively 550 nm near a stratigraphic depth of 150 m Fig. 1*C*). This reflects a color change from a mixture of purple and red below 150 m, to predominantly red and virtually no purple above this stratigraphic level. Similar color changes are evident from the color representation of the core lithostratigraphy Fig. 1*B*), and the stratigraphic order of core photographs and the CIE values are available at https://osf.io/5vd8u/. Torrent Q:8 and Barrón 32) suggest the wavelength band shifts between Q:9 535 nm and 570 nm according to the specific surface area of single hematite grains. As hematite size increases, visible color lies within the blue-indigo-violet part of the spectrum because absorption occurs near the wavelength range of yellow. The

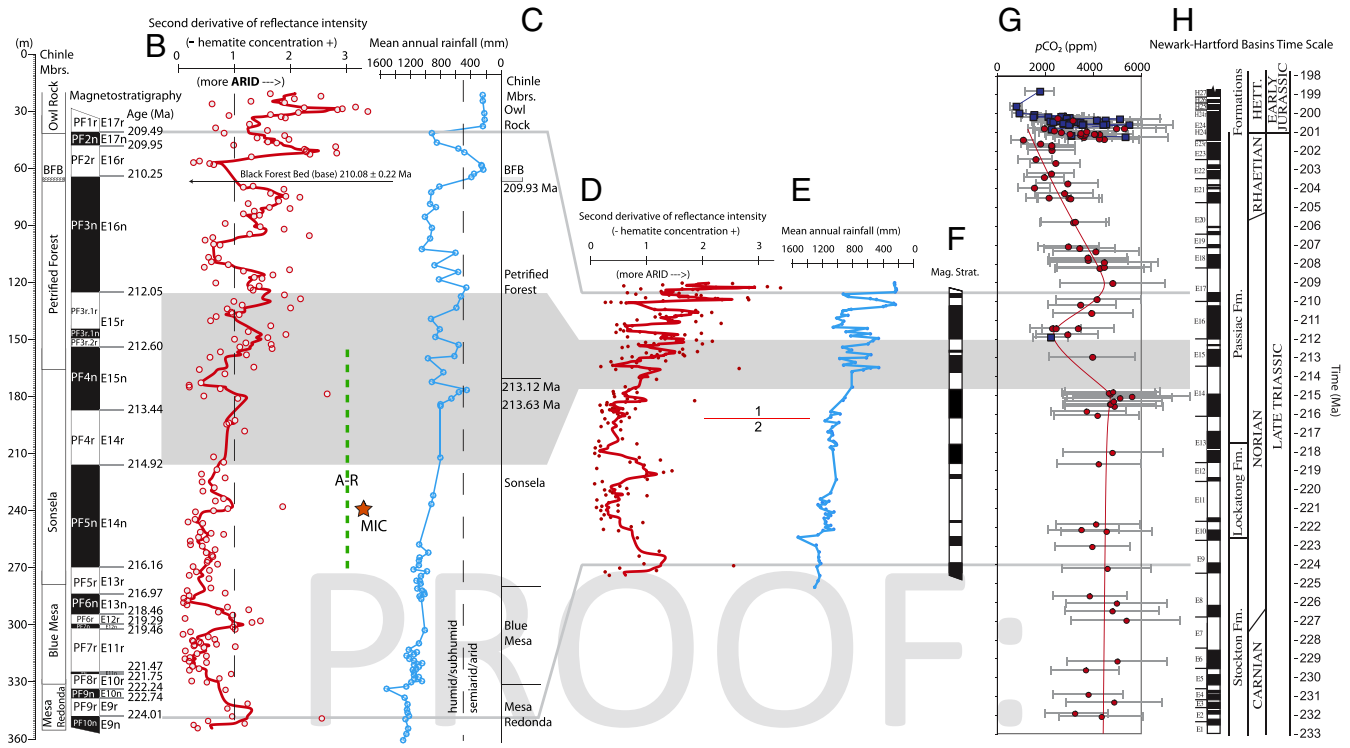

Fig. 2. (*A*) Magneto-chronostratigraphy of the Chinle Formation in PFNP core 1A (18, 25). BFB is the stratigraphic position of the Black Forest Bed dated within the core (19). (*B*) Second derivative values at 535 to 570 nm of the intensity of hematite reflectance measured using DRS (this study). The thick red line is a six-point moving average of the (red circles) measured values. Hematite concentrations increase (more arid) toward the right. The green dashed line is the interval correlative to the Adamanian–Revueltian (A–R) biotic change (18, 24). The orange star is the date of the Manicouagan impact crater (MIC) (59, 60). (*C*) Q:26 Outcrop data of variations in mean annual rainfall (millimeters) from the CIA–K transfer function, with radioisotopic zircon dates for the BFB and volcaniclastic horizons in the upper Sonsela Member (22, 26). (*D*) Hematite data stretched to time using the two accumulation rate intervals of ref. 18, with 1 being 30 m/My and 2 being 10 m/My. (*E*) Mean annual rainfall stretched to time as in *D*. (*F*) Chile magnetostratigraphy stretched to time as in *D*. (*G*) Late Triassic and Early Jurassic atmospheric pCO_2 (57). The gray bars represent the range of possible pCO_2 values modeled using the *z* test score distribution from Monte Q:27 Carlo simulations, with the red trend line placed by the eye (57). (*H*) Newark–Hartford astrochronostratigraphic polarity time scale (APTS) (17, 56). The gray Q:28 shading indicates the magnetostratigraphic interval (chrons E14 and E15) that constrains the drawdown of pCO_2 at 215 to 212 Ma. The gray lines indicate the interval of the Chinle magnetostratigraphy correlative to the Newark–Hartford APTS.

expression of red/yellowish-red hematite is associated with smaller grain size and absorption between 535 and 550 nm 32). Elemental concentrations *SI Appendix*, *Supplementary Information Text* and Table S3) suggest our observed trends are not primarily due to Al substitution for Fe within the hematite octahedral structure.

The up-core shift to absorption values of 550 nm indicates reddening and suggests a decrease in hematite grain size, consistent with increasing aridity 33, 34). In accordance with these changes is the progressive increase of hematite concentration upwardly through the core Fig. 2*B*). The initial onset of this long-term increase gradually begins within the Sonsela Member, constrained to about 217 to 213 Ma, and continues into the lower Owl Rock Member at 209.49 Ma Fig. 2 *A* and *B*). Superimposed on this trend are a number of cycle-like oscillations that appear to begin near a stratigraphic core depth of 180 m within the upper Sonsela Member at 213 Ma. However, there is a paucity of paleosols) DRS measurements between 214.92 and 213.44 Ma, raising the possibility that the changes began earlier. The amplitudes of the oscillations apparently increase progressively through time, with the most pronounced changes in amplitude appearing after 210 Ma. In the lower part of the core, transient shifts toward higher hematite concentrations occur near 224.01 Ma Mesa Redonda Member), 219.29 Ma Blue Mesa Member), and at about 215.5 Ma within the mid/lower Sonsela Member Fig. 2 *A* and *B*).

The DRS record from the Chinle core Fig. 2*B*) shares similar trends with the Late Triassic record of mean annual rainfall Fig. 2*C*) that is based on the CIA-K data collected in ref. 22 from Chinle outcrops. Each paleoenvironmental record indicates a long-term shift toward greater aridity beginning near 215 Ma Fig. 2 *B* and *C*), and both records demonstrate cycle-like oscillations which commence in the upper Sonsela Member and culminate with large amplitude changes in the Owl Rock Member. These similarities between the core and outcrop data indicate that the hematite record captures changes to the Late Triassic monsoon occurring over the Colorado Plateau. Given the sensitivity of the Pangaean monsoon to astronomical climate forcing 8, 35), it is possible that the cycle-like oscillations of both records reflect changes in precipitation governed by orbital mechanics. The seemingly abrupt onset of these oscillations and subsequent amplitude change is currently under consideration, but it has been suggested that the differential expression of astronomical forcing in Pangaean records may vary with latitudinal climatic zones 36). The applicability of this hypothesis to our study is supported by the northward drift of Laurentia and associated movement of the Colorado Plateau into subtropical latitudes Fig. 1*A*), which may also explain the progressive increase of aridity indicated by both records Fig. 2 *B* and *C*). Regardless of their origins, correlating individual cycle-like oscillations between the outcrop and core records is complicated by changes in sediment accumulation processes across the basin

28) and uncertainties in the compilations of local sections 37) coupled with the lower sample density for the outcrop data.

Another consideration is that portions of the outcrop paleoenvironmental signal may also be affected by diagenetic alterations of various ages. For example, acid tests 22) indicate an anomalous lack of calcium carbonate in the matrix of paleosols within an 20-m interval directly below the Black Forest Bed. These observations suggest that ancient minerals used to construct the CIA-K may have been leached from the matrix. The area of sampling is overlain by the Neogene Bidahochi Formation with its own paleoweathering profile at the contact with Chinle. This may account for a rather attenuated outcrop paleoenvironmental signal derived from paleosols in the upper Petrified Forest Member Fig. 2*C*).

It should be noted that the parameterization of the CIA-K data only affords a reconstruction of mean annual rainfall and does not possess the resolution to infer seasonality or other nuanced aspects of a climate regime 38). In contrast, hematite production is predicted to be strongly linked to seasonal moisture/temperature changes in the soil environment 33, 39). In the lower part of the formation, increases of hematite near 224.01 Ma Mesa Redonda) and 219.29 Ma Blue Mesa) and within the mid/lower Sonsela at about 215.5 Ma Fig. 2*B*) may represent episodic changes to the seasonality regime that are inherent to but not obviously expressed by the outcrop record of mean annual rainfall Fig. 2*C*).

Discussion

Red beds of the Chinle Formation contain both specularite and pigmentite, with the latter often represented by multiple generations of varying grain sizes and magnetic properties 7, 40). The paleomagnetic overprint for red beds appears to reside with late diagenetic components associated with pigmentary hematite phases 9, 16). There is more uncertainty, however, regarding the existence of a primary pigmentite phase that may contribute to the characteristic remanent magnetization. The thermal unblocking spectra of pigmentary phases overlap with that of the detrital remanence carried by specularite and may extend up to temperatures closer to hematite s Neel temperature 1, 2, 9). This makes it challenging to deconvolve the pigmentite and specularite signals and use paleomagnetic data to test for the presence of primary pigmentite and distinguish it from late diagenetic phases. Our DRS data indicate pigmentite that formed close to the time of the initial deposition of the red beds. If some of this pigmentite has a coarse enough grain size, then it may have a magnetic remanence that was acquired at nearly the same time as the characteristic remanent magnetization carried by detrital specularite grains. Further work integrating DRS and magnetic methods would help to test these expectations.

Pedogenic hematite derives from the dehydration and solid-state rearrangement of ferrihydrite and is thus favored by dry/warm environments 33, 34). Monsoonal climates are amenable for pedogenic hematite because iron III) production is facilitated by the aeration of soil pore spaces during dry seasons 39) and aerobic respiration of soil organic material 41). Pedogenic hematite often is competitive with goethite, which forms out of solution from Fe ions under more humid conditions 33, 34, 42, 43). No definitive evidence for a goethite presence was indicated by rock magnetic experiments and thermal demagnetization patterns for Chinle core samples 18, 19). Goethite and hematite competition is also constrained by soil pH and organic matter 44); however, the related effects of temperature, moisture, pH, and organics are difficult to isolate. In the lower part of the Chinle Formation when mean annual rainfall was higher, vegetation probably increased and caused soil pH to acidify. This would have been a less favorable environment for pedogenic hematite 33, 44). On the other hand, when the climate was arid in the uppermost Sonsela Member, Petrified Forest, and Owl Rock members, pedogenic calcium carbonate becomes more abundant and vegetation was plausibly reduced 22, 27). Calcium carbonate acts as a buffering agent that stabilizes soil pH. Hematite fluctuations in the upper part of the formation may therefore be more of a direct measure of soil temperature/moisture 45).

The wetting and drying necessary for pigmentite formation may come from a climate system that is not monsoonal. For example, soil-formed hematite is common under a Mediterranean climate, often derived from maghemite through a series of mineral transformations 46). However, this type of midlatitude climate appears to have been unlikely given that the paleo area never drifts out of the tropics/subtropics 47). Monsoons predominate over large continental areas of Earth within these latitudes 48, 49). It is the seasonality that drives hydrolysis and the liberation of Fe ions from clays and other silicates. Moisture is therefore needed to derive the Fe ions that form ferrihydrite. Seasonal dryness is needed for the desiccation step that forms pigmentite from ferrihydrite 33). If the climate is too dry or lacks a prominent wet season, the derivation of Fe ions is suppressed 50, 51).

The timing of the pigmentite formation within soils and its acquisition of a chemical remanent magnetization is not well constrained and is an issue receiving ongoing research 2, 52, 53). Studies on monsoonal/tropical soils suggest that hematite forms over timescales ranging from seasonal to 100 ky 42, 51, 54, 55). Given the sedimentation rates calculated for the Chinle Formation about 1 to 3 cm per 1,000 y) 18, 19, 28), the soils are integrating high-frequency climate changes that we cannot detect with our methods. Certainly, diachronous soil mineralization processes are occurring down the soil profile, within the subsurface. However, because of the slow sedimentation rate and the scale of the pigmentite climate trends consistent with the outcrop record of mean annual rainfall Fig. 2), we do not consider that the timing of pigment formation has introduced a bias into the first-order directional shifts in our record. Nonetheless, other factors may be at play, such as the differences in mudstone composition and the exposure time of floodplains i.e., paleosol maturation rates) already noted for the Chinle Formation 22, 26).

An overall upward increase in hematite concentration through the core is consistent with interpretations that the Chinle Formation records a progressive decline in Late Triassic monsoonal precipitation 24, 26, 27). This drying has been linked to a rain shadow caused by orogeny along the Cordilleran magmatic arc 22). However, northward drift of the Colorado Plateau as part of Laurentia from humid latitudes of 7° at 220 Ma into the arid subtropics 16°) by nearly 200 Ma Fig. 1*A*) provides a simpler mechanism supported by paleolatitudinal data 47, 56). In either case, what the datasets cannot help to elucidate is whether the drying trend was a result of decreased wet season rainfall or increased aridity during the dry seasons, or whether there was a change in the number and length of wet/dry seasons each year. Moreover, the CIA-K data Fig. 2*C*) are interpreted as a proxy for mean annual precipitation and therefore are not considered to give insight into seasonality. That is why the interpretation that the monsoon "collapsed" 22, 26) is not directly substantiated by the CIA-K data. These data cannot discriminate whether the climate change derives from a progressively dryer monsoon or whether the defining aspect of a monsoon i.e., seasonal changes in wind vectors) ceased to exist and was replaced by something different. Our pigmentite record is fundamentally different from the CIA-K data; as discussed above, the soil-formed pigmentite has greater sensitivity to the disparities of soil moisture that arise from monsoonal seasonality. The interpretation that the pigmentite and the CIA-K data carry similar yet different aspects of the same monsoonal climate may account from some of the mismatch between the two records, such as

near the stratigraphic level of the Black Forest Bed Fig. 2). Nonetheless, we interpret that the Late Triassic monsoon did not collapse but monsoonal seasonality remained active, albeit drier, through upper Chinle deposition. An orographic rain shadow may have coincided with the already changing monsoon and exacerbated the mounting disparities between wet and dry seasons but appears to have not been related to a wholesale climate shift, nor is it necessary, given the phenomena known to have occurred.

Magnetostratigraphic correlations between the Chinle record and the Newark–Hartford basins of northeastern North America demonstrate that the Colorado Plateau aridification covered by our record was penecontemporaneous with a transient drawdown and then increase of Late Triassic atmospheric pCO_2 Fig. 2*D*). While a drawdown is thought to be caused by enhanced silicate weathering due to drift of a greater area of Pangaea into the tropical belt 57), which positions the Colorado Plateau within the arid subtropics, that mechanism does not seem consistent with the transient pCO_2 drawdown at around 210 Ma. In any case, consistency in records between the Newark–Hartford basins and the Colorado Plateau is expected if the arid climate shift was due to Pangaea-wide mechanisms, like continental drift, rather than local orographic effects. Our record of hematite increase is consistent with a more nuanced scenario of the interaction between the documented pCO_2 changes and the northward drift of this part of Pangaea. As the Colorado Plateau area drifted from a more humid belt into the semiarid belt, soil hematite increased but at a relatively low rate as pCO_2 dropped Fig. 2*D*). As this transient reversed at about 211 Ma, soil hematite increased at its fastest rate as the effects of increasing pCO_2 and northward drift aligned in direction. This scenario could be tested by the study of Chile paleosol sequences that would be expected to have dropping levels of hematite as the effects of a more sustained drop in pCO_2 countered the effects of further northward drift after 209 Ma. An indication that this might actually be the case is the more purple and drab colors seen in the overlying Owl Rock Member that fully overlaps in time with the sustained pCO_2 drawdown from 209 Ma to 202 Ma, terminated by the abrupt pCO_2 rise caused by the eruptions of the Central Atlantic Magmatic Province 58).

An $^{40}Ar/^{39}Ar$ age of 215.40 ± 0.16 Ma 59) for the Manicouagan impact melt sheet of Canada is within the age range of the onset of the long-term drying trend at 215 Ma Fig. 2 *A* and *B*). However, we have difficulty envisioning a simple model of how an impact could have generated the aridity, sustained it, or enhanced it for over 6 My and also caused the observed hematite climate oscillations beginning at 213 Ma. Furthermore, the Chinle climate record has no unusual variability at 215 Ma. The modest increase of hematite at about 215.5 Ma core depth of 240 m) might be a possible signature of a bolide impact; however, it is nonunique because there are other outliers near 224.01 and 219.29 Ma Fig. 2 *A* and *B*). No remarkable change in mean annual rainfall coincides with the date of the Manicouagan impact Fig. 2*C*).

Although a detailed chronology for the Adamanian–Revueltian biotic turnover is yet to be established, as is its precise correlation to the core, magneto-chronostratigraphic results for PFNP-core 1A constrain the turnover at 216 to 213 Ma 18), bringing it into closer temporal agreement with the timing of the Manicouagan impact 59, 60). If the Manicouagan impact and the biotic turnover are related 61), then monsoonal climate change appears not to be the link between them. The Chinle climate record provides no compelling evidence of an impact-induced event between 216 and 213 Ma. The most dramatic inflections of the hematite climate record are what we interpret as a gradual increase of aridity starting at 215 Ma and the onset of climate oscillations at 213 Ma. Through this time, the biotic turnover may have been influenced by monsoonal rainfall changes derived from the northward tectonic drift of Pangaea into the arid subtropical latitudes, although a more dramatic change caused by the Manicouagan bolide impact cannot be ruled out.

Conclusion

Study of PFNP-core 1A of the Chinle Formation Arizona) adds to the growing evidence that hematite—particularly the "pigmentite" phase that gives red beds their characteristic colors—is a valid recorder of the Late Triassic climate history of Pangaea. Spectrophotometry measurements of the pigmentite concentrations in Chinle red beds indicate rising aridity and increased oscillatory climate change through the Late Triassic of the Colorado Plateau. This is parsimoniously explained by the northward drift of the Laurentian part of Pangaea into the arid subtropical latitudes. The timing of the monsoonal changes coincides with the Adamanian–Revueltian biotic turnover dated to 216 to 213 Ma and thus may have contributed to this event. No significant climate inflection was observed near the date of the Manicouagan impact structure in Canada. If the impact and biotic turnover were related, then the monsoon appears not to be the direct link between the two.

Data Availability. All data used for this study can be found within the *SI Appendix*.

ACKNOWLEDGMENTS. DRS measurements were made by the Fe Oxide Lab (NSF Grant 1818805 to C.J.L.) of the Department of Earth and Planetary Sciences of Rutgers University. We thank Sean Kinney and Clara Chang for facilitating the X-ray fluorescence measurements. We thank the Colorado Plateau Coring Project (CPCP) Phase 1 team members for their collaborative efforts. We are grateful for discussions with Dennis Kent and his insights into the ideas presented here. CPCP Phase 1 was funded in part by NSF collaborative grant EAR 0958976 (P.E.O Co-PI), and P.E.O. acknowledges support from the Lamont Climate Center.

1. E. Irving, N. D. Opdyke, The palaeomagnetism of the bloomsburg red beds and its possible application to the tectonic history of the appalachians. *Geophys J Int* **9**, 153–167 (1965).
2. Z. Jiang *et al*., Acquisition of chemical remanent magnetization during experimental ferrihydrite–hematite conversion in Earth-like magnetic field—Implications for paleomagnetic studies of red beds. *Earth Planet Sci Lett* **428**, 1–10 (2015).
3. M. Kerker, P. Scheiner, D. D. Cooke, J. P. Kratohvil, Absorption index and color of colloidal hematite. *J Colloid Interface Sci* **71**, 176–187 (1979).
4. F. Hund, Inorganic pigments: Bases for colored, uncolored, and transparent products. *Angew Chem Int Ed Engl* **20**, 723–730 (1981).
5. Q. Liu *et al*., Quantifying grain size distribution of pedogenic magnetic particles in Chinese loess and its significance for pedogenesis: Pedogenic particles in loess. *J Geophys Res* , 10.1029/2005JB003726 (2005).
6. Ö. Özdemir, D. J. Dunlop, Hysteresis and coercivity of hematite: Hysteresis and coercivity of hematite. *J Geophys Res Solid Earth* **119**, 2582–2594 (2014).
7. D. W. Collinson, The role of pigment and specularite in the remanent magnetism of red sandstones. *Geophys J Int* **38**, 253–264 (1974).
8. P. E. Olsen, D. V. Kent, Milankovitch climate forcing in the tropics of Pangaea during the late triassic. *Palaeogeogr Palaeoclimatol Palaeoecol* **122**, 1–26 (1996).
9. N. L. Swanson Hysell, L. M. Fairchild, S. P. Slotznick, Primary and secondary red bed magnetization constrained by fluvial intraclasts. *J Geophys Res Solid Earth* **124**, 4276–4289 (2019).
10. F. B. Van Houten, Origin of red beds A review-1961-1972. *Annu Rev Earth Planet Sci* **1**, 39–61 (1973).
11. Walker *et al*., Nature and origin of hematite in the moenkopi formation (triassic), Colorado plateau: A contribution to the origin of magnetism in red beds. *J Geophys Res* **86**, 317 (1981).
12. R. A. Berner, Goethite stability and the origin of red beds. *Geochim Cosmochim Acta* **33**, 267–273 (1969).
13. M. E. Beck, R. F. Burmester, B. A. Housen, The red bed controversy revisited: Shape analysis of Colorado plateau units suggests long magnetization times. *Tectonophysics* **362**, 335–344 (2003).
14. R. D. Elmore, A. R. Muxworthy, M. Aldana, Remagnetization and chemical alteration of sedimentary rocks. *Geol Soc Lond Spec Publ* **371**, 1–21 (2012).
15. D. V. Kent, P. E. Olsen, W. K. Witte, Late Triassic-earliest Jurassic geomagnetic polarity sequence and paleolatitudes from drill cores in the Newark rift basin, eastern North America. *J Geophys Res* **100**, 14965–14998 (1995).

16. L. Tauxe, D. V. Kent, N. D. Opdyke, Magnetic components contributing to the NRM of Middle Siwalik red beds. *Earth Planet Sci Lett* **47**, 279–284 (1980).
17. P. E. Olsen, D. V. Kent, B. Cornet, W. K. Witte, R. W. Schlische, High-resolution stratigraphy of the Newark rift basin (early Mesozoic, eastern North America). *Geol Soc Am Bull* **108**, 40–77 (1996).
18. D. V. Kent *et al*., Magnetochronology of the Entire Chinle formation (Norian Age) in a scientific drill core from petrified forest National park (Arizona, USA) and implications for regional and global correlations in the Late Triassic. *Geochem Geophys Geosyst* **20**, 4654–4664 (2019).
19. D. V. Kent *et al*., Empirical evidence for stability of the 405-kiloyear Jupiter-Venus eccentricity cycle over hundreds of millions of years. *Proc Natl Acad Sci U S A* **115**, 6153–6158 (2018).
20. R. F. Hayes *et al*., Modeling the dynamics of a late triassic vertebrate extinction: The adamanian/revueltian faunal turnover, petrified forest National park, Arizona, USA. *Geology* **48**, 318–322 (2020).
21. S. G. Lucas, Global Triassic tetrapod biostratigraphy and biochronology. *Palaeogeogr Palaeoclimatol Palaeoecol* **143**, 347–384 (1998).
22. Nordt *et al*., Collapse of the late triassic megamonsoon in western equatorial pangea, present-day American southwest. *Geol Soc Am Bull* **127**, 1798–1815 (2015).
23. P. E. Olsen, D. V. Kent, J. H. Whiteside, Implications of the Newark Supergroup-based astrochronology and geomagnetic polarity time scale (Newark-APTS) for the tempo and mode of the early diversification of the Dinosauria. *Earth Environ Sci Trans R Soc Edinb* **101**, 201–229 (2010).
24. W. G. Parker, J. W. Martz, The late triassic (Norian) adamanian–Revueltian tetrapod faunal transition in the Chinle Formation of petrified forest National park, Arizona. *Earth Environ Sci Trans R Soc Edinb* **101**, 231–260 (2010).
25. P. E. Olsen, J. Geissman, D. V. Kent, G. E. Gehrels, Colorado Plateau Coring Project, phase I (CPCP-I): A continuously cored, globally exportable chronology of triassic continental environmental change from western North America. *Sci Drill* **24**, 15–40 (2018).
26. S. C. Atchley *et al*., A linkage among Pangean tectonism, cyclic alluviation, climate change, and biologic turnover in the Late Triassic: The record from the Chinle formation, Southwestern United States. *J Sediment Res* **83**, 1147–1161 (2014).
27. L. H. Tanner, S. G. Lucas, "Calcareous paleosols of the Upper Triassic Chinle Group, Four Corners region, southwestern United States: Climatic implications" in *Special Paper 416: Paleoenvironmental Record and Applications of Calcretes and Palustrine Carbonates*, (Geological Society of America, 2006), vol. 416, pp. 53–74.
28. C. Rasmussen *et al*., U-Pb zircon geochronology and depositional age models for the upper triassic Chinle Formation (petrified forest National park, Arizona, USA): Implications for late triassic paleoecological and paleoenvironmental change. *Geol Soc Am Bull* **130**, 20 (2020).
29. C. J. Lepre, Constraints on Fe oxide Formation in monsoonal Vertisols of pliocene Kenya using rock magnetism and spectroscopy. *Geochem Geophys Geosyst* **20**, 4998–5013 (2019).
30. G. R. Rossman, "Why hematite is red: Correlation of optical absorption intensities and magnetic moments of Fe3+ minerals" in *Mineral Spectroscopy: A Tribute to Roger G Bums* (1996), vol. 6.
31. A. C. Scheinost, A. Chavernas, V. Barron, J. Torrent, Use and limitations of second-derivative diffuse reflectance spectroscopy in the visible to near-infrared range to identify and quantify Fe oxide minerals in soils. *Clays Clay Miner* **46**, 528–536 (1998).
32. J. Torrent, V. Barrón, The visible diffuse reflectance spectrum in relation to the color and crystal properties of hematite. *Clays Clay Miner* **51**, 309–317 (2003).
33. U. Schwertmann, "Occurrence and formation of iron oxides in various pedoenvironments" in *Iron in Soils and Clay Minerals*, J. W. Stucki, B. A. Goodman, U. Schwertmann, Eds. (Springer Netherlands, 1988), pp. 267–308.
34. U. Schwertmann, Transformation of hematite to goethite in soils. *Nature* **232**, 624–625 (1971).
35. P. E. Olsen *et al*., Mapping solar system chaos with the geological orrery. *Proc Natl Acad Sci U S A* **116**, 10664–10673 (2019).
36. J. H. Whiteside, D. S. Grogan, P. E. Olsen, D. V. Kent, Climatically driven biogeographic provinces of Late Triassic tropical Pangea. *Proc Natl Acad Sci U S A* **108**, 8972–8977 (2011).
37. J. W. Martz, W. G. Parker, Revised lithostratigraphy of the Sonsela member (Chinle Formation, upper triassic) in the southern part of petrified forest National park, Arizona. *PLoS One* **5**, e9329 (2010).
38. N. D. Sheldon, G. J. Retallack, S. Tanaka, Geochemical climofunctions from North American soils and application to paleosols across the eocene oligocene boundary in Oregon. *J Geol* **110**, 687–696 (2002).
39. B. A. Maher, Palaeoclimatic records of the loess/palaeosol sequences of the Chinese Loess Plateau. *Quat Sci Rev* **154**, 23–84 (2016).
40. D. W. Collinson, Origin of remanent magnetization and initial susceptibility of certain red sandstones. *Geophys J Int* **9**, 203–217 (1965).
41. J. M. Bigham, R.W. Fitzpatrick, "Iron oxides" in *Soil Mineralogy with Environmental Applications*, D. G. Schulze, Ed. (Soil Science Society of America, 2002), pp. 323–366.
42. X. Long, J. Ji, W. L. Balsam, Rainfall-dependent transformations of iron oxides in a tropical saprolite transect of Hainan Island, South China: Spectral and magnetic measurements. *J Geophys Res* **116**, 1–15 (2011).
43. J. Torrent, V. Barrón, Q. Liu, Magnetic enhancement is linked to and precedes hematite formation in aerobic soil. *Geophys Res Lett* **33**, L02401 (2006).
44. U. Schwertmann, E. Murad, Effect of pH on the formation of goethite and hematite from ferrihydrite. *Clays Clay Miner* **31**, 277–284 (1983).
45. R. Zhang, J. Nie, Goethite concentration variations in the red clay sequence on the Chinese loess plateau: Variations of goethite in the red clay. *Geochem Geophys Geosyst* **18**, 4179–4185 (2017).
46. J. Torrent, Q. S. Liu, V. Barrón, Magnetic minerals in Calcic Luvisols (Chromic) developed in a warm Mediterranean region of Spain: Origin and paleoenvironmental significance. *Geoderma* **154**, 465–472 (2010).
47. D. V. Kent, E. Irving, Influence of inclination error in sedimentary rocks on the Triassic and Jurassic apparent pole wander path for North America and implications for Cordilleran tectonics. *J Geophys Res* **115**, B10103 (2010).
48. S. E. Nicholson, Climate and climatic variability of rainfall over eastern africa: Climate over eastern africa. *Rev Geophys* **55**, 590–635 (2017).
49. J. E. Kutzbach, R. G. Gallimore, Pangaean climates: Megamonsoons of the megacontinent. *J Geophys Res* **94**, 3341 (1989).
50. J. C. Larrasoaña *et al*., Source-to-sink magnetic properties of NE saharan dust in eastern mediterranean marine sediments: Review and paleoenvironmental implications. *Front Earth Sci* , 10.3389/feart.2015.00019 (2015).
51. W. Balsam, J. Ji, J. Chen, Climatic interpretation of the Luochuan and Lingtai loess sections, China, based on changing iron oxide mineralogy and magnetic susceptibility. *Earth Planet Sci Lett* **223**, 335–348 (2004).
52. Z. Jiang *et al*., A new model for transformation of ferrihydrite to hematite in soils and sediments. *Geology* **46**, 987–990 (2018).
53. D. Bilardello, S. K. Banerjee, M. W. R. Volk, J. A. Soltis, R. L. Penn, Simulation of natural iron oxide alteration in soil: Conversion of synthetic ferrihydrite to hematite without artificial dopants, observed with magnetic methods. *Geochem Geophys Geosyst* **21**, e2020GC009037 (2020).
54. J. Ji, W. Balsam, J. Chen, Mineralogic and climatic interpretations of the luochuan loess section (China) based on diffuse reflectance spectrophotometry. *Quat Res* **56**, 23–30 (2001).
55. Ji *et al*., High resolution hematite/goethite records from Chinese loess sequences for the last glacial-interglacial cycle: Rapid climatic response of the East Asian Monsoon to the tropical Pacific. *Geophys Res Lett* **31** (2004).
56. Kent *et al*., Astrochronostratigraphic polarity time scale (APTS) for the Late Triassic and Early Jurassic from continental sediments and correlation with standard marine stages. *Earth Sci Rev* **166**, 153–180 (2017).
57. M. F. Schaller, J. D. Wright, D. V. A. Kent, 30 Myr record of Late Triassic atmospheric pCO_2 variation reflects a fundamental control of the carbon cycle by changes in continental weathering. *Geol Soc Am Bull* **127**, 661–671 (2014).
58. M. F. Schaller, J. D. Wright, D. V. Kent, Atmospheric PCO_2 perturbations associated with the central atlantic magmatic Province. *Science* **331**, 1404–1409 (2011).
59. S. J. Jaret *et al*., Context matters–Ar–Ar results from in and around the Manicouagan impact structure, Canada: Implications for martian meteorite chronology. *Earth Planet Sci Lett* **501**, 78–89 (2018).
60. J. Ramezani *et al*., The Manicouagan impact melt rock: A proposed standard for the intercalibration of U-Pb and 40Ar/39Ar isotopic systems. *Geochim Cosmochim Acta Suppl* **69**, A321 (2005).
61. M. R. Rampino, Relationship between impact-crater size and severity of related extinction episodes. *Earth Sci Rev* **201**, 102990 (2020).